

Accepted Manuscript

Instantaneous fluorescent probe for the specific detection of H₂S

Xianfeng Lin, Xiuhong Lu, Junliang Zhou, Hang Ren, Xiaochun Dong, Weili Zhao, Zhongjian Chen



PII: S1386-1425(19)30099-X

DOI: <https://doi.org/10.1016/j.saa.2019.01.085>

Reference: SAA 16771

To appear in: *Spectrochimica Acta Part A: Molecular and Biomolecular Spectroscopy*

Received date: 31 October 2018

Revised date: 11 January 2019

Accepted date: 28 January 2019

Please cite this article as: X. Lin, X. Lu, J. Zhou, et al., Instantaneous fluorescent probe for the specific detection of H₂S, *Spectrochimica Acta Part A: Molecular and Biomolecular Spectroscopy*, <https://doi.org/10.1016/j.saa.2019.01.085>

This is a PDF file of an unedited manuscript that has been accepted for publication. As a service to our customers we are providing this early version of the manuscript. The manuscript will undergo copyediting, typesetting, and review of the resulting proof before it is published in its final form. Please note that during the production process errors may be discovered which could affect the content, and all legal disclaimers that apply to the journal pertain.

Instantaneous fluorescent probe for the specific detection of H₂S

Xianfeng Lin,^a Xiuhong Lu,^a Junliang Zhou,^a Hang Ren,^a Xiaochun Dong,^{*,a} Weili Zhao,^{*,a,b} and Zhongjian Chen^{*,c}

^a School of Pharmacy, Fudan University, 826 Zhangheng Road, Shanghai, 201203, P. R. China

^b Key Laboratory for Special Functional Material of the Ministry of Education, Henan University, Kaifeng, 475004, P. R. China

^c Shanghai Dermatology Hospital, Shanghai, 200443, P. R. China

ABSTRACT

Novel cyanine-based fluorescent probes for the detection of H₂S were developed. The probes developed are stable under physiological conditions. The water soluble fluorescent probe **2** displayed ultrafast and specific response to H₂S displaying NIR fluorescence of 115-fold turn-on with the detection limit of 11 nM without assistance of organic solvent or surfactant. Cell imaging experiments indicated that probe **2** was cell-permeable and was able to detect H₂S sensitively in lysosomes. Moreover, our probe was able to detect H₂S intrinsically produced H₂S through enzymatic/non-enzymatic biosynthetic pathway from Cys/GSH. Moreover, we applied probe **2** to detect H₂S in living mice and demonstrated the fast metabolism of H₂S. Thus, probe **2** shows great promise as a reporter for H₂S.

Keywords: fluorescent probe, H₂S, lysosome-targeted

1. Introduction

Recent biological reports have established the important role of H₂S, and new evidence suggests that H₂S may emerge as the most important gasotransmitter which regulates many important physiological functions in the cardiovascular, nervous, endocrine, immune, gastrointestinal systems [1, 2]. Furthermore, H₂S serves as a scavenger for endogenous reactive oxygen species (ROS) [3]. However, abnormal H₂S production is associated with various human diseases including the symptoms of Down syndrome [4], hypertension [5], and diabetes [6]. Physiologically, endogenous H₂S is primarily produced from cysteine or cysteine derivatives in the mitochondria or cytosol catalyzed by cystathionine- γ -lyase (CSE), cystathionine- β -synthase (CBS), and 3-mercaptopyruvate sulphurtransferase (3MST) [7]. On the other hand, glutathione and polysulfides can be transformed to H₂S through non-enzymatic pathway [8]. Once generated, H₂S undergoes complex catabolism (with half-life of a few minutes to be metabolized) through its interactions with reactive sulfur, oxygen, nitrogen species (RSONs), cellular oxidants, and protein transition-metal centers [8]. H₂S in an aqueous solution has a pK_a of 7.0. It freely permeates plasma membranes, and undergoes fast metabolism in the mitochondria *via* the sulfide oxidation pathway [9]. In subcellular level, there is some evidence that both CBS and CSE are localized to the cytoplasm, whereas 3MST is localized predominantly to the mitochondria [1, 7]. The complicated reactions involving H₂S make the detection of H₂S in biological systems very difficult, therefore, the biologically relevant concentrations of H₂S have been debated [10-12].

The volatile, lipophilic, diffusive, and highly reactive nature (with half-life of a few minutes to be metabolized), and complicated reactions involving H₂S make the detection of H₂S in biological systems very difficult. Various H₂S-mediated processes such as reduction (reduction of azides or reduction of nitro groups), nucleophilic addition, nucleophilic aromatic substitution (aryl nitro thiolysis), replacement of copper, and coordinative-based approach have been applied for the probe design [7,

13-19]. For easy use for the detection of H₂S in living systems, the chemosensing agent should meet at least the following four criteria: (1) act rapidly (within seconds) under mild conditions; (2) be sensitive for detection under near physiological conditions; (3) show minimal or no interference by other anions in blood serum; (4) be functional in aqueous solutions and blood plasma [8]. Unfortunately, the existing probes hardly satisfy all of these criteria, hampering further application of them to tackle biological issues [20-24]. Only a few examples could detect H₂S relatively fast, but are poorly water-soluble [25-29]. Some probes are organelle-targeted (such as mitochondria [30-35], and lysosome [36-40]). However, they frequently required long recognition time. The lack of ideal probe for the measurement of H₂S limited advances in the field and many of its underlying molecular events remain unknown, especially in the subcellular level.

To address the challenging responding rate and to favorite *in vivo* applications, cyanine type dyes were chosen to screen H₂S responsive probes and we were happy to find that dinitrophenol ether of cyanine dye (**1**) was capable of fast response to H₂S. Further optimization led to the discovery of more favorable water-soluble version (**2**) as shown in Chart 1.

2. Experimental Section

2.1 Materials and Instrumentation

All reagents were purchased from commercial suppliers and used without further purification. Solvents used were purified by standard methods prior to use. All of the intermediates were purified by silica gel chromatography using an ISCO CombiFlash chromatography instrument. All of the final compounds were purified by preparative HPLC (prep-HPLC) on a reversed-phase column using a Waters X-Bridge Phenyl (30 mm × 100 mm, 5 μm) or OBD RP18 (30 mm × 100 mm, 5 μm) column under acidic conditions (A, 0.1% formic acid in H₂O; B, 0.1% formic acid in acetonitrile) or basic conditions (A, 0.1% ammonia in H₂O; B, acetonitrile). ¹H NMR spectra were recorded on a NMR spectra were obtained using Bruker AVANCE 400 MHz spectrometer. ¹H NMR chemical shifts (δ) are given in ppm (s = singlet, d = doublet, t

= triplet, q = quartet, m = multiplet) downfield from Me₄Si, determined by chloroform ($\delta = 7.26$ ppm). ¹³C NMR spectra were recorded on a Bruker AVANCE 100 MHz spectrometer. ¹³C NMR chemical shifts (δ) are reported in ppm with the internal CDCl₃ at δ 77.0 as standard, respectively. All the photophysical characterization experiments were carried out at 25 °C. Absorption spectra were collected on a Hitachi U-2900 double beam UV-vis spectrophotometer. Fluorescence spectra were collected on Hitachi F-2500 fluorescence spectrophotometer with slit widths to be 10 nm and 10 nm for excitement and emission respectively. Phosphate buffer saline (PBS, 10 mM, pH 7.2) was used to prepare all aqueous solutions. To test the fluorescence responses of the probes towards reactive species, aliquots of probe stock solutions were diluted with PBS and treated with analytes to make sure both probes and analytes were kept at desired final concentrations. ESI-HRMS (high resolution mass spectrometry) spectra were obtained on Agilent Technologies 6530 Accurate-Mass Q-TOF LC-MS. LC-MS (ESI, low resolution mass spectrometry) spectra were obtained on Waters X-Bridge Phenyl or OBD RP18 column and Waters AcQuiry (PDA Detector, SQ Detector, ELS Detector, Sample Manager-FL, Column Manager, Binary Solvent Manager, MassLynx).

All cell lines obtained from American Typical Cell Collection (ATCC) and the Type Culture Collection of the Chinese Academy of Sciences were maintained in respective growth medium which were recommended by the vendors. Cell lines cultured in needed medium (from Invitrogen) with 10% (vol/vol) fetal bovine serum qualified (from Gibco, FBS, #10099-141, origin Australia) at 37 °C in a humidified incubator containing 5% CO₂. Cell Counting Kit-8 (CCK8, cat. no. CK04-20, Kumamoto, Japan) was purchased from Dojindo Molecular Tech. Lysosome tracker green and Mito-tracker green were purchased from Thermofisher.

2.2 Preparation and Characterization of Probes

Synthesis of 4-(2',4'-dinitrophenoxy) benzene-1,3-dicarbaldehyde

Commercially available 1-fluoro-2,4-dinitro-benzene (300 mg, 2 mmol) was added to a stirring solution of commercial available

4-hydroxybenzene-1,3-dicarbaldehyde (372 mg, 2 mmol) and potassium carbonate (414 mg, 3 mmol) in N,N-dimethylformamide (5 mL) at room temperature. After 1 hour, TLC indicated that the start materials consumed. The mixture was diluted with ethyl acetate (50 mL) and washed with water (30 × 3 mL). The organic phase was dried over Na₂SO₄, evaporated in vacuo and the residue was purified by flash column chromatography eluting with petroleum/EtOAc (3:1) to afford 4-(2',4'-dinitrophenoxy) benzene-1,3-dicarbaldehyde (537 mg, yield: 85%) as pale yellow solid. ¹H NMR (400MHz, DMSO-*d*₆) δ = 10.33 (s, 1H), 10.10 (s, 1H), 8.97 (d, J=2.8 Hz, 1H), 8.56 (dd, J=2.8, 9.2 Hz, 1H), 8.50 (d, J=2.2 Hz, 1H), 8.26 (dd, J=2.1, 8.5 Hz, 1H), 7.57 (d, J=9.2 Hz, 1H), 7.46 (d, J=8.6 Hz, 1H). ¹³C NMR (100MHz, DMSO-*d*₆) δ = 192.02, 189.01, 160.17, 153.32, 143.61, 140.85, 136.84, 133.82, 132.32, 130.47, 127.48, 122.76, 122.64, 120.98.

Synthesis of probe 1

The mixture of 4-(2',4'-dinitrophenoxy) benzene-1,3-dicarbaldehyde (95 mg, 0.30 mmol), 1,2,3,3-tetramethylindolium iodide (181 mg, 0.60 mmol) and NaOAc (74 mg, 0.90 mmol) in Ac₂O (5 mL) was stirred at 80 °C for 2 hours under Ar atmosphere and monitored by LC-MS. After completion, the reaction mixture was concentrated by evaporation under reduced pressure. The residue was diluted with 2 mL DMF, 2 mL HOAc, and purified by preparative-HPLC (grad. 10%-90 ACN in water, 20 min) to afford probe **1** (148 mg, 48%). ¹H NMR (400MHz, Methanol-*d*₄) δ = 9.06 (d, J=2.8 Hz, 1H), 9.00 (d, J=2.0 Hz, 1H), 8.66 (d, J=2.8 Hz, 1H), 8.65 - 8.62 (m, 2H), 8.52 (s, 1H), 8.40 (dd, J=2.3, 8.8 Hz, 1H), 7.95 - 7.88 (m, 2H), 7.86 - 7.79 (m, 2H), 7.77 - 7.66 (m, 6H), 7.41 (d, J=8.8 Hz, 1H), 4.31 (s, 3H), 4.29 (s, 3H), 1.93 (s, 6H), 1.86 (s, 6H). ¹³C NMR (100MHz, Methanol-*d*₄) δ = 182.73, 182.69, 157.32, 152.50, 151.01, 150.94, 144.26, 143.89, 143.82, 141.83, 140.87, 135.25, 132.65, 132.26, 130.23, 130.00, 129.47, 129.30, 129.20, 126.36, 122.65, 122.63, 122.06, 119.17, 115.23, 114.99, 52.94, 52.91, 52.90, 35.24, 34.60, 24.88, 24.86. HRMS (ESI): calc'd for C₃₈H₃₆N₄O₅ [M]²⁺ 314.13374, measured 314.13378.

Synthesis of 2,3,3-trimethyl-1-(3-sulfopropyl) indolium inner salt

A mixture of commercially available 2,3,3-trimethylindolenine (15.9 g, 10.0 mmol) and 1,3-propanesultone (12.2 g, 10.0 mmol) in toluene (200 mL) was refluxed overnight. After cooling, the precipitate was filtered and washed with ethyl acetate. The product 2,3,3-trimethyl-1-(3-sulfopropyl) indolium inner salt (21.3 g, 76%) was collected as red powder and was used in the next reaction without further purification.

Synthesis of probe 2

The mixture of 4-(2',4'-dinitrophenoxy) benzene-1,3-dicarbaldehyde (105 mg, 0.33 mmol), 2,3,3-trimethyl-1-(3-sulfopropyl) indolium inner salt (197 mg, 0.70 mmol) and NaOAc (33 mg, 0.40 mmol) in Ac₂O (5 mL) was stirred at 80 °C for 2 hours under Ar atmosphere and monitored by LC-MS. After completion, the reaction mixture was concentrated by evaporation under reduced pressure. The residue was diluted with 2 mL H₂O, 2 mL HOAc, and purified by preparative-HPLC (grad. 10%–90 ACN in water, 20 min) to afford probe **2** (172 mg, 62%). ¹H NMR (400 MHz, DMSO-*d*₆) δ = 9.45 (d, *J*=1.6 Hz, 1H), 9.00 (d, *J*=2.8 Hz, 1H), 8.72 (dd, *J*=1.7, 8.8 Hz, 1H), 8.65 (d, *J*=16.4 Hz, 1H), 8.59 (dd, *J*=2.8, 9.2 Hz, 1H), 8.50 - 8.43 (m, 1H), 8.37 - 8.29 (m, 1H), 8.19 - 8.05 (m, 3H), 7.91 - 7.87 (m, 2H), 7.71 - 7.62 (m, 5H), 7.50 (d, *J*=8.8 Hz, 1H), 5.10 - 4.93 (m, 4H), 2.78 - 2.64 (m, 4H), 2.35 - 2.19 (m, 4H), 1.89 (s, 6H), 1.74 (s, 6H). ¹³C NMR (100 MHz, DMSO-*d*₆) δ = 182.70, 182.12, 156.98, 153.10, 152.12, 144.77, 144.61, 144.27, 143.49, 141.35, 141.30, 140.79, 136.33, 133.71, 133.08, 130.50, 130.21, 129.78, 129.63, 126.88, 123.66, 123.60, 122.65, 122.36, 120.31, 116.90, 116.14, 115.93, 114.77, 53.06, 52.81, 49.09, 47.58, 47.49, 46.48, 46.31, 26.18, 25.33. HRMS (ESI): calc'd for C₄₂H₄₂N₄O₁₁S₂ [M+2H]²⁺ 422.12185, measured [M+2H]²⁺ 422.12166.

2.3 Confocal Imaging Experiments

Hela or HepG2 cells were seeded at 1 × 10⁵ cells per ml in Dulbecco's Modified Eagle Medium (DMEM) containing 10% (v/v) fetal bovine serum, 1% penicillin/streptomycin at 37 °C in a humidified incubator with 5% CO₂. 24 hours later, cells were treated with different conditions as described in the figure legend, and

then washed three times with 0.1 M Hank's buffer. All confocal fluorescence images were acquired by an LSM710 confocal microscope with a 40 × objective (Carl Zeiss).

2.4 Fluorescence Imaging in Mice

All procedures were carried out in compliance with the Guide for the Care and Use of Laboratory Animal Resources and the National Research Council. The bioimaging experiments on living mice utilized the Kunming mice (Sino-British SIPPR/BK Lab. Animal Ltd, China) in vivo imaging system equipped with a sensitive Charge Coupled Device (CCD) camera, with the excitation at 590 nm and the 680 nm emission filter. Healthy mice (20–25 g) were used, and animals had free access to food and water. The mice were anesthetized, and the abdominal fur was removed. Mice without any treatment was kept as a control; i) NaHS (20 mM, 0.2 mL) was injected into the peritoneal cavity of the mouse; then the probe (50 μM, 0.2 mL) was injected into the peritoneal cavity of the mice; ii) NaHS (20 mM, 0.2 mL) was injected into the peritoneal cavity of the mouse; 10 min later, the probe (50 μM, 0.2 mL) was injected into the peritoneal cavity of the mice; iii) the probe (50 μM, 0.2 mL) was injected into the peritoneal cavity of the mouse; 10 min later, NaHS (20 mM, 0.2 mL) was injected into the peritoneal cavity of the mice. Images were taken after incubation for different times, 1 min, 2 min, 3 min, 4 min, 5 min, 6 min, 7 min, 8 min, 9 min, 10min, 20 min, 30 min, 40 min, 50 min, 60 min with the excitation filter at 590 nm and the emission filter set at 680 nm; iv) the probe (50 μM, 0.2 mL) was injected into the peritoneal cavity of the mouse.

3. Results and Discussion

3.1 Syntheses of Probes

The preparations of the probes were very straight forward (Scheme 1). 2,3,3-trimethylindolenium salt functionalized at 1 position with methyl or sulfopropyl was reacted with 4-(2',4'-dinitrophenoxy) benzene-1,3-dicarbaldehyde made from 1-fluoro-2,4-dinitro-benzene and 4-hydroxybenzene-1,3-dicarbaldehyde in the presence of acetic anhydride and sodium acetate led to the desired probe **1** or **2** in good yield (Scheme 1). The required 2,3,3-trimethylindolenium salt functionalized at

1 position sulfopropyl as inner salt may be easily prepared by refluxing 2,3,3-trimethylindolenine with 1,3-propanesultone in toluene. The reference dye of probe **2** (herein designated as dye **3**) was also synthesized easily as shown in Scheme S1 simply started from 4-hydroxybenzene-1,3-dicarbaldehyde. The well-known mechanism of the reaction-based fluorescent probe capped as dinitrophenoxy ether for the detection of H₂S was that thiolation of the dinitrobenzene portion in ipso attack to release the parent dye **3** [41].

3.2 Colorimetric and Fluorimetric Assays in Solution

The absorption spectra of probes **1** (10 μM) and **2** in PBS solution (10 mM, pH = 7.2) at 25 °C were nearly identical with absorption maximum at 400 nm ($\epsilon = 35300 \text{ M}^{-1} \text{ cm}^{-1}$ for **1**, and $43200 \text{ M}^{-1} \text{ cm}^{-1}$ for **2**, respectively) viewed as pale yellow color with naked eyes (Figure 1). Both probes (**1** and **2**) are non-fluorescent ($\Phi_f < 0.01$) due to photo-induced electron transfer (PET) from the fluorophore to the electronic sink of dinitrobenzene moiety [42]. Upon addition of NaHS (50 μM), two new absorption bands for both **1** (λ_{max} at 468 nm and 565 nm, respectively) and **2** (λ_{max} at 476 nm and 590 nm, respectively) appeared. The color turned into gray accordingly viewed with naked eyes. Under irradiation with UV light, red color fluorescence was clearly generated after addition of NaHS.

The fluorescence produced by probe **1** in the presence of NaHS has the emission maximum of 665 nm with fairly fast response and nice fluorescence enhancement (118-fold). It was discovered that probe **2** displayed more intensive emission at maximum of 680 nm with ultrafast response which reached to half of the saturated intensities within 4 seconds and finished within 2 minutes while maintaining excellent fluorescence enhancement of 115-fold (Figure 2). The fast response is extremely important considering the quick metabolism (with half-life of a few minutes) and volatile nature of H₂S in biological systems. As far as we know, NIR fluorescent H₂S probes with such a rapid and remarkable fluorescence changes without assistance of organic solvent or surfactant are extremely rare in the literature (Table S2). Therefore,

the spontaneously responsive probe **2** with large Stokes shift (90 nm) was selected for further evaluation.

To determine whether our probe **2** was selective for H₂S detection, we carried out the fluorescence measurements with 1 equiv. of the probe to react with 5 equiv. of NaHS in PBS solution (10 mM, pH = 7.2) at 25 °C in comparison with 100 equiv. of various potential interferents *e.g.* gas transmitter (NO), various oxidants (NaClO, H₂O₂, KO₂), nucleophile (KSCN), various thio species (NaHSO₄, Na₂S₂O₃, Cys, Hcy, GSH), and other common amino acids *e.g.* alanine (Ala), methionine (Met), lysine (Lys), glutamine (Gln), serine (Ser), etc. The fluorescence intensities collected at 680 nm with the excitation of 590 nm of light were collected in Figure 3. To our delight, our probe was demonstrated to specifically respond to H₂S and none of other analytes could interfere the detection of H₂S. Therefore, probe **2** displayed desirable selectivity and speed.

Our next experiment was to find the sensitivity of our probe developed. Therefore, concentration-dependent response profile determined in PBS was provided in Figure 4. Linearly proportional to analyte concentration was observed for probe **2** to be in the range of 1–10 μM. The detection limit was calculated to be around 11 nM.

For the reaction mechanism, it is well established that thiolation of the capping moiety to release the parent dye (herein dye **3**) was generally followed (Figure S1). Our MS studies shown in Fig. S1 indicated that the desired dye **3** was released by thiolation of probe **1** with the moiety of 2,4-dinitrothiophenol produced. Once the capping moiety was removed, the PET effect was terminated and therefore ignited the fluorescence of the dye [41].

3.3 Imaging Hydrogen Sulfide in Living Cells

So far, the ultrafast, sensitive and specific characteristics of probe **2** performed in PBS buffer without assistance of organic solvent were fairly favorable for the detection of H₂S. To favorite imaging applications, toxicity studies using CCK-8 assays on the fluorescence response of probe **2** to NaHS were carried out. Various cells used for the toxicity studies (including HCT16, HT29, A549, H1944, MCF-7,

MDA-MB-468, MDA-MB-231, PANC1, etc) indicated that good toleration with IC_{50} greater than $80 \mu\text{M}$ (Table S1 and Figure S2). Both the data and figures displayed in Table S1 and Figure S2 suggested the low toxicity of our probe.

To demonstrate that probe **2** could be applied for H_2S detection in live cells, confocal fluorescent imaging experiments with probe **2** were subsequently carried out and the results were shown in Figure S3 with HeLa cells. The dim images in red channel for intrinsic H_2S suggested that the level in native live HeLa cells was low (Figure S3). Astonishingly, when external H_2S was added, clear red images were found mostly in spherical shape which was suspected to be lysosome-targeted. The same phenomena were noticed in HepG2 cells as well (Figure S4). The observations suggested that probe **2** was cell permeable and could detect H_2S in live cells with most probably in lysosomes.

To find solid evidence that our probe **2** could detect H_2S in lysosomes, colocalization studies were subsequently performed using commercially available Mito-Tracker Green and Lyso-Tracker Green as standards. Both HeLa and HepG2 cells were adopted for the colocalization studies. Cells were initially incubated with known subcellular targeting dye (Lyso-Tracker Green) for 20 min and then treated with probe **2** for 10 min. After further incubation with NaHS for 10 min, the confocal fluorescence images were recorded and the images were illustrated in Figure 5. The fluorescence images produced using **2** overlapped relatively well with the region stained with Lyso-Tracker Green both in HeLa (Figure 5A, 0.83) and HepG2 (Figure 5B, 0.68) cells. The overlapped parts viewed as spherical-shaped were thus expected to be lysosome-targeted area. In stark contrast, the generated fluorescent images overlapped poorly with Mito-Tracker Green from the merged images (Figure S5).

Since the non-fluorescent nature of probe **2** prohibited investigation of the subcellular distribution with direct fluorescence imaging, we therefore investigated the distribution the parent dye (**3**) of probe **2** instead as alternative supporting information (Figure S6). The colocalization of parent dye **3** with Lyso-Tracker Green in HeLa cells with overlap coefficient of 0.67 (Figure S6) suggested that the dye **3** was

most probably lysosome-targeted. The confocal fluorescence imaging experiments strongly suggested that probe **2** was able to detect H₂S elegantly inside living cells and mostly probably in lysosomes.

In addition to supplementing cells with extraneous sources of sulphide, we put our efforts to test whether we can detect intrinsically produced H₂S through enzymatic/non-enzymatic biosynthetic pathway. Cys as a substrate of CBS and reduced glutathione (GSH) as a typical non-enzymatic supplier were adopted (Figure S7). Imaging experiments were carried out with probe **2** (10 μM), as previously described, and cells were incubated with either 100 μM Cys or GSH. After addition of thiol species and 1 hour of incubation, further incubation with probe **2** for 10 min elicited significant response in both cases. On the other hand, further stimulation with PMA for ROS generation after thiol addition, subsequent incubation with probe **2** eliminated the fluorescence.

3.4 Fluorescence Imaging in Mice

To explore the potential usage of probe **2** as an *in vivo* imaging tool, we applied it to H₂S detection in living mice (Figure 6). Briefly, probe **2** was injected 30 s after administrating *i.p.* injection of NaHS (20 mM) in mice and images were taken at various period of time. Strong fluorescence was visualized immediately (1 min) and the intensity declined quickly over extended time (Figure 6, upper row). In contrast, once probe **2** was injected 10 min after administrating *i.p.* injection of NaHS (20 mM) in mice, much weaker fluorescence was detected (Figure 6, middle row). When NaHS was injected after administrating *i.p.* injection of probe **2**, very strong intensity of fluorescence was visualized and longer sustain of fluorescence was noted (Figure 6, bottom row). Therefore, the results suggested that NaHS metabolized fairly rapidly *in vivo* and the dye generated also metabolized. Administrating only probe **2** led to weak fluorescence signals (Figure S8), which may indicate that even intrinsic H₂S may possibly be detected by probe **2**, thus reflected the good sensitivity of our probe.

4. Conclusion

In conclusion, a novel water soluble cyanine-based fluorescent probe for H₂S was developed. The probe developed is stable under physiological conditions. Such a probe responded ultrafast and specifically to H₂S with the detection limit of 11 nM in PBS buffer. To the best of our knowledge, our NIR fluorescent probe with such large Stokes shift, instantaneous and specific response to H₂S in PBS buffer without assistance of organic solvent or surfactant is unique compared to the recently reported probes (Table S2). Moreover, our probe was lysosome-targeted and was able to detect H₂S even for the intrinsically produced H₂S (both enzymatic/non-enzymatic biosynthesized). Pleasantly, we successfully applied probe **2** to detect H₂S in living mice and demonstrated the fast metabolism of H₂S. Thus, the probe shows great promise as a reporter for H₂S. We anticipate that these results would inspire and encourage researchers to elucidate the role of H₂S in biology and pharmacology.

Acknowledgements

This research was supported by National Natural Science Foundation of China (21372063, 81601173).

References

- [1] C. Szabó, Hydrogen sulphide and its therapeutic potential, *Nat. Rev. Drug Discov.* 6 (2007) 917-935.
- [2] R. Wang, Two's company, three's a crowd: can H₂S be the third endogenous gaseous transmitter?, *FASEB J* 16 (2002) 1792-1798.
- [3] B.D. Paul, S.H. Snyder, H₂S signalling through protein sulfhydration and beyond, *Nat. Rev. Mol. Cell Biol.* 13 (2012) 499-507.
- [4] B.K. Czyzewski, D.-N. Wang, Identification and characterization of a bacterial hydrosulphide ion channel, *Nature* 483 (2012) 494-497.
- [5] A. Stein, S.M. Bailey, Redox biology of hydrogen sulfide: Implications for physiology, pathophysiology, and pharmacology, *Redox Biol.* 1 (2013) 32-39.
- [6] H. Kimura, Metabolic turnover of hydrogen sulfide, *Front. Physiol.* 3 (2012) 101.

- [7] V.S. Lin, W. Chen, M. Xian, C.J. Chang, Chemical probes for molecular imaging and detection of hydrogen sulfide and reactive sulfur species in biological systems, *Chem. Soc. Rev.* 44 (2015) 4596-4618.
- [8] H. Peng, Y. Cheng, C. Dai, A.L. King, B.L. Predmore, D.J. Lefer, B. Wang, A fluorescent probe for fast and quantitative detection of hydrogen sulfide in blood, *Angew. Chem., Int. Ed.* 50 (2011) 9672-9675.
- [9] Y. Qian, J. Karpus, O. Kabil, S.-Y. Zhang, H.-L. Zhu, R. Banerjee, J. Zhao, C. He, Selective fluorescent probes for live-cell monitoring of sulphide, *Nat. Commun.* 2 (2011) 495.
- [10] A.R. Lippert, E.J. New, C.J. Chang, Reaction-based fluorescent probes for selective imaging of hydrogen sulfide in living cells, *J. Am. Chem. Soc.* 133 (2011) 10078-10080.
- [11] V.S. Lin, A.R. Lippert, C.J. Chang, Cell-trappable fluorescent probes for endogenous hydrogen sulfide signaling and imaging H₂O₂-dependent H₂S production, *Proc. Natl. Acad. Sci. U. S. A.* 110 (2013) 7131-7135.
- [12] S.K. Bae, C.H. Heo, D.J. Choi, D. Sen, E.-H. Joe, B.R. Cho, H.M. Kim, A ratiometric two-photon fluorescent probe reveals reduction in mitochondrial H₂S production in Parkinson's disease gene knockout astrocytes, *J. Am. Chem. Soc.* 135 (2013) 9915-9923.
- [13] F. Yu, X. Han, L. Chen, Fluorescent probes for hydrogen sulfide detection and bioimaging, *Chem. Commun.* 50 (2014) 12234-12249.
- [14] V.S. Lin, C.J. Chang, Fluorescent probes for sensing and imaging biological hydrogen sulfide, *Curr. Opin. Chem. Biol.* 16 (2012) 595-601.
- [15] H. Peng, W. Chen, Y. Cheng, L. Hakuna, R. Strongin, B. Wang, Thiol reactive probes and chemosensors, *Sensors* 12 (2012) 15907-15946.
- [16] M.H. Lee, J.S. Kim, J.L. Sessler, Small molecule-based ratiometric fluorescence probes for cations, anions, and biomolecules, *Chem. Soc. Rev.* 44 (2015) 4185-4191.
- [17] X. Zhou, S. Lee, Z. Xu, J. Yoon, Recent progress on the development of chemosensors for gases, *Chem. Rev.* 115 (2015) 7944-8000.

- [18] N. Kumar, V. Bhalla, M. Kumar, Recent developments of fluorescent probes for the detection of gasotransmitters (NO, CO and H₂S), *Coord. Chem. Rev.* 257 (2013) 2335-2347.
- [19] M. Strianese, C. Pellicchia, Metal complexes as fluorescent probes for sensing biologically relevant gas molecules, *Coord. Chem. Rev.* 318 (2016) 16-28.
- [20] B. Ke, W. Wu, W. Liu, H. Liang, D. Gong, X. Hu, M. Li, Bioluminescence probe for detecting hydrogen sulfide in vivo, *Anal. Chem.* 88 (2016) 592-595.
- [21] X. Jin, S. Wu, M. She, Y. Jia, L. Hao, B. Yin, L. Wang, M. Obst, Y. Shen, Y. Zhang, J. Li, Novel fluorescein-based fluorescent probe for detecting H₂S and its real applications in blood plasma and biological imaging, *Anal. Chem.* 88 (2016) 11253-11260.
- [22] J. Cao, R. Lopez, J.M. Thacker, J.Y. Moon, C. Jiang, S.N.S. Morris, J.H. Bauer, P. Tao, R.P. Mason, A.R. Lippert, Chemiluminescent probes for imaging H₂S in living animals, *Chem. Sci.* 6 (2015) 1979-1985.
- [23] Y. Qian, L. Zhang, S. Ding, X. Deng, C. He, X.E. Zheng, H.-L. Zhu, J. Zhao, A fluorescent probe for rapid detection of hydrogen sulfide in blood plasma and brain tissues in mice, *Chem. Sci.* 3 (2012) 2920-2923.
- [24] K. Zhang, J. Zhang, Z. Xi, L.Y. Li, X. Gu, Q.Z. Zhang, L. Yi, A new H₂S-specific near-infrared fluorescence-enhanced probe that can visualize the H₂S level in colorectal cancer cells in mice, *Chem. Sci.* 8 (2017) 2776-2781.
- [25] E. Karakus, M. Ucuncu, M. Emrullahoglu, Electrophilic cyanate as a recognition motif for reactive sulfur species: selective fluorescence detection of H₂S, *Anal. Chem.* 88 (2016) 1039-1043.
- [26] Q. Fu, G. Chen, Y. Liu, Z. Cao, X. Zhao, G. Li, F. Yu, L. Chen, H. Wang, J. You, In situ quantification and evaluation of ClO⁻/H₂S homeostasis in inflammatory gastric tissue by applying a rationally designed dual-response fluorescence probe featuring a novel H⁺-activated mechanism, *Analyst* 142 (2017) 1619-1627.
- [27] J. Liu, Y.-Q. Sun, J. Zhang, T. Yang, J. Cao, L. Zhang, W. Guo, A ratiometric fluorescent probe for biological signaling molecule H₂S: fast response and high selectivity, *Chem.-Eur. J.* 19 (2013) 4717-4722.

- [28] Y. Chen, C. Zhu, Z. Yang, J. Chen, Y. He, Y. Jiao, W. He, L. Qiu, J. Cen, Z. Guo, A ratiometric fluorescent probe for rapid detection of hydrogen sulfide in mitochondria, *Angew. Chem., Int. Ed.* 52 (2013) 1688-1691.
- [29] L. Wei, Z. Zhu, Y. Li, L. Yi, Z. Xi, A highly selective and fast-response fluorescent probe for visualization of enzymatic H₂S production in vitro and in living cells, *Chem. Commun.* 51 (2015) 10463-10466.
- [30] Roopa, N. Kumar, V. Bhalla, M. Kumar, Development and sensing applications of fluorescent motifs within the mitochondrial environment, *Chem. Commun.* 51 (2015) 15614-15628.
- [31] J. Liu, X. Guo, R. Hu, X. Liu, S. Wang, S. Li, Y. Li, G. Yang, Molecular engineering of aqueous soluble triarylboron-compound-based two-photon fluorescent probe for mitochondria H₂S with analyte-induced finite aggregation and excellent membrane permeability, *Anal. Chem.* 88 (2016) 1052-1057.
- [32] Y.L. Pak, J. Li, K.C. Ko, G. Kim, J.Y. Lee, J. Yoon, Mitochondria-targeted reaction-based fluorescent probe for hydrogen sulfide, *Anal. Chem.* 88 (2016) 5476-5481.
- [33] N. Velusamy, A. Binoy, K.N. Bobba, D. Nedungadi, N. Mishra, S. Bhuniya, A bioorthogonal fluorescent probe for mitochondrial hydrogen sulfide: new strategy for cancer cell labeling, *Chem. Commun.* 53 (2017) 8802-8805.
- [34] L. Zhou, D. Lu, Q. Wang, S. Liu, Q. Lin, H. Sun, Molecular engineering of a mitochondrial-targeting two-photon in and near-infrared out fluorescent probe for gaseous signal molecules H₂S in deep tissue bioimaging, *Biosens. Bioelectron.* 91 (2017) 699-705.
- [35] X. Feng, T. Zhang, J.-T. Liu, J.-Y. Miao, B.-X. Zhao, A new ratiometric fluorescent probe for rapid, sensitive and selective detection of endogenous hydrogen sulfide in mitochondria, *Chem. Commun.* 52 (2016) 3131-3134.
- [36] X.J. Zou, Y.C. Ma, L.E. Guo, W.X. Liu, M.J. Liu, C.G. Zou, Y. Zhou, J.F. Zhang, A lysosome-targeted fluorescent chemodosimeter for monitoring endogenous and exogenous hydrogen sulfide by in vivo imaging, *Chem. Commun.* 50 (2014) 13833-13836.

- [37] Z. Wu, D. Liang, X. Tang, Visualizing hydrogen sulfide in mitochondria and lysosome of living cells and in tumors of living mice with positively charged fluorescent chemosensors, *Anal. Chem.* 88 (2016) 9213-9218.
- [38] Y. Liu, F. Meng, L. He, K. Liu, W. Lin, A dual-site two-photon fluorescent probe for visualizing lysosomes and tracking lysosomal hydrogen sulfide with two different sets of fluorescence signals in the living cells and mouse liver tissues, *Chem. Commun.* 52 (2016) 7016-7019.
- [39] X. Zhang, H. Tan, Y. Yan, Y. Hang, F. Yu, X. Qu, J. Hua, Targetable N-annulated perylene-based colorimetric and ratiometric near-infrared fluorescent probes for the selective detection of hydrogen sulfide in mitochondria, lysosomes, and serum, *J. Mater. Chem. B* 5 (2017) 2172-2180.
- [40] T. Liu, Z. Xu, D.R. Spring, J. Cui, A lysosome-targetable fluorescent probe for imaging hydrogen sulfide in living cells, *Org. Lett.* 15 (2013) 2310-2313.
- [41] X. Cao, W. Lin, K. Zheng, L. He, A near-infrared fluorescent turn-on probe for fluorescence imaging of hydrogen sulfide in living cells based on thiolysis of dinitrophenyl ether, *Chem. Commun.* 48 (2012) 10529-10531.
- [42] Y. Tang, D. Lee, J. Wang, G. Li, J. Yu, W. Lin, J. Yoon, Development of fluorescent probes based on protection–deprotection of the key functional groups for biological imaging, *Chem. Soc. Rev.* 44 (2015) 5003-5015.

Chart 1. The Structures of Fluorescent Probes Developed.

Scheme 1. Syntheses of Fluorescent Probes.

Figure 1. Absorption and fluorescence spectra ($\lambda_{ex} = 590$ nm) of 10 μ M of probes **1** (a, b) and **2** (c, d) prior to (black) and after (red) addition of NaHS (50 μ M) in PBS solution (10 mM, pH = 7.2) at 25 °C (Insets in c and d: the color change under room light and UV irradiation viewed by naked eyes respectively).

Figure 2. Time-dependent fluorescence responses ($\lambda_{ex} = 590$ nm) monitored from 4 seconds at emission maxima for probes **1** and **2** (10 μ M each) after addition of NaHS (50 μ M) in PBS solution (10 mM, pH = 7.2) at 25 °C.

Figure 3. Fluorescence responses of probe **2** (10 μ M) to various amino acids, oxidants (1 mM each) in comparison with NaHS (50 μ M) at room temperature monitored at 680 nm ($\lambda_{ex} = 590$ nm) in PBS buffer (10 mM, pH = 7.2). Data were recorded at 2 minutes after addition of various analytes.

Figure 4. Fluorescence intensities changes of probe **2** (10 μ M) in the presence of increasing concentrations of NaHS (0, 0.1, 0.5, 1, 2, 3, 4, 5, 6, 7, 8, 9, 10 μ M) in PBS solution (10 mM, pH = 7.2) at 25 °C ($\lambda_{ex}/\lambda_{em} = 590/680$ nm).

Figure 5. Confocal fluorescence images of HeLa (row A) and HepG2 cells (row B) with multiple labels. Cells incubated with Lyso-Tracker Green (100 nM for A, B) for 20 min and probe **2** (10 μ M) for 10 min, and then incubated with NaHS (100 μ M) for 10 min. All cells were incubated at 37 °C and all cells were rinsed three times with 0.1 M Hank's buffer before imaging (A1/B1: green channel images; A2/B2: red channel images; A3/B3: merged images, A4/B4: Fluorescent intensity profiles of the regions of interest in merged image).

Figure 6. In vivo imaging of H₂S in living mice. Upper row: i.p. injection of probe **2** (50 μ M, 0.2 mL) right after administrating of NaHS (20 mM, 0.2 mL); Middle row: i.p. injection of probe **2** (50 μ M, 0.2 mL) 10 min after administrating of NaHS (20 mM, 0.2 mL); Bottom row: i.p. injection of NaHS (20 mM, 0.2 mL) after

administering of probe **2** (50 μ M, 0.2 mL). Mice without injection were used as control in all experiments.

ACCEPTED MANUSCRIPT

Highlights

- A novel water soluble cyanine-based NIR fluorescent Probe **2** for H₂S.
- Responded ultrafast and specifically to H₂S with the detection limit of 11 nM in PBS buffer.
- Lysosome-targeted and capable of detecting endogenous, exogenous, and even the intrinsically produced H₂S (both enzymatic/non-enzymatic biosynthesized).
- Successfully applied to detect H₂S in living mice and demonstrated the fast metabolism of H₂S.

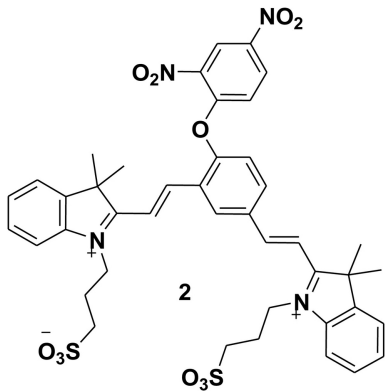
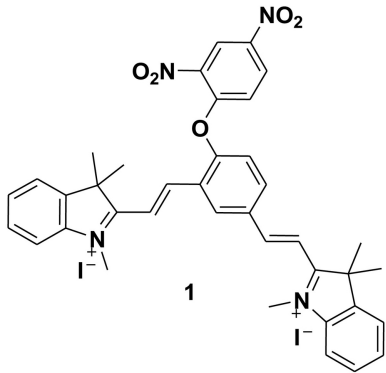


Figure 1

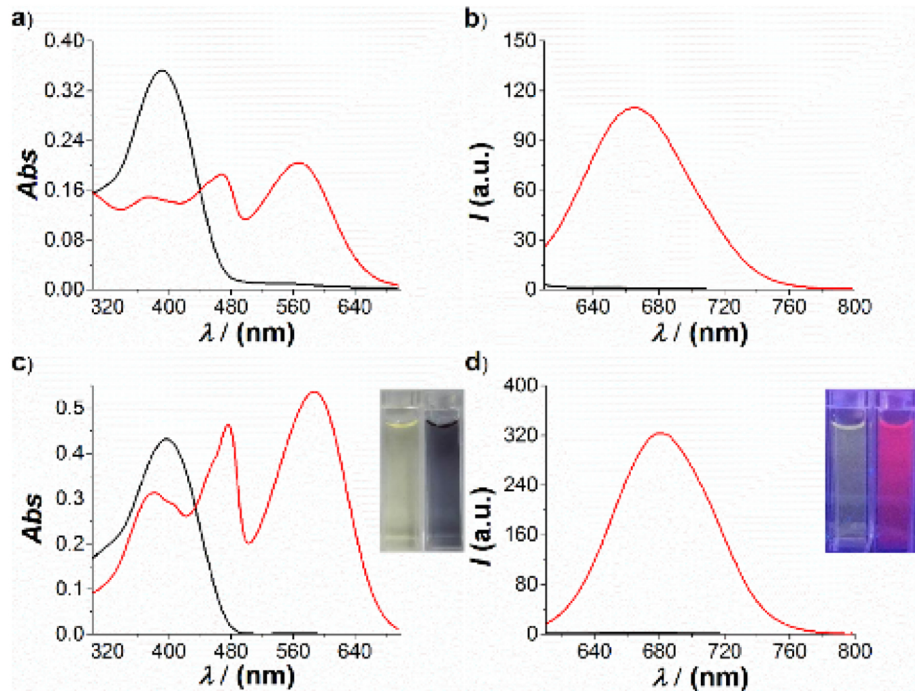


Figure 2

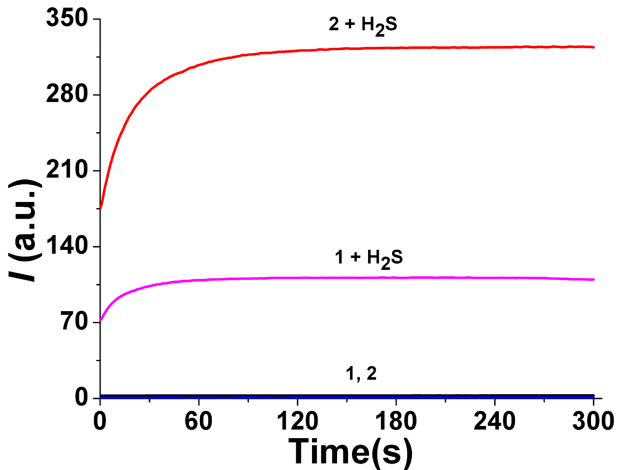


Figure 3

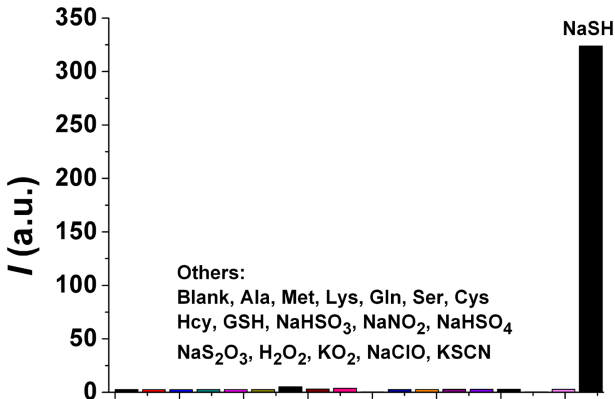


Figure 4

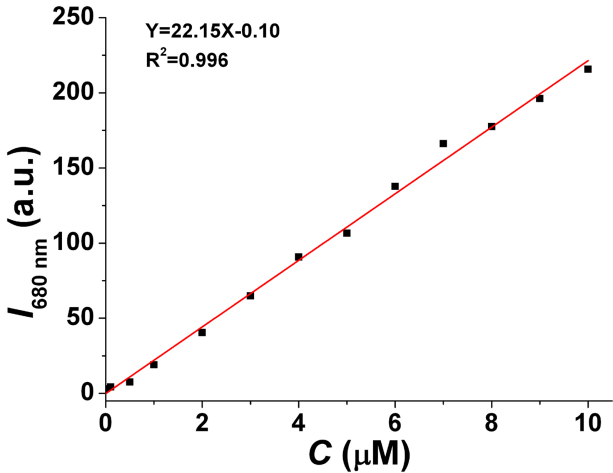


Figure 5

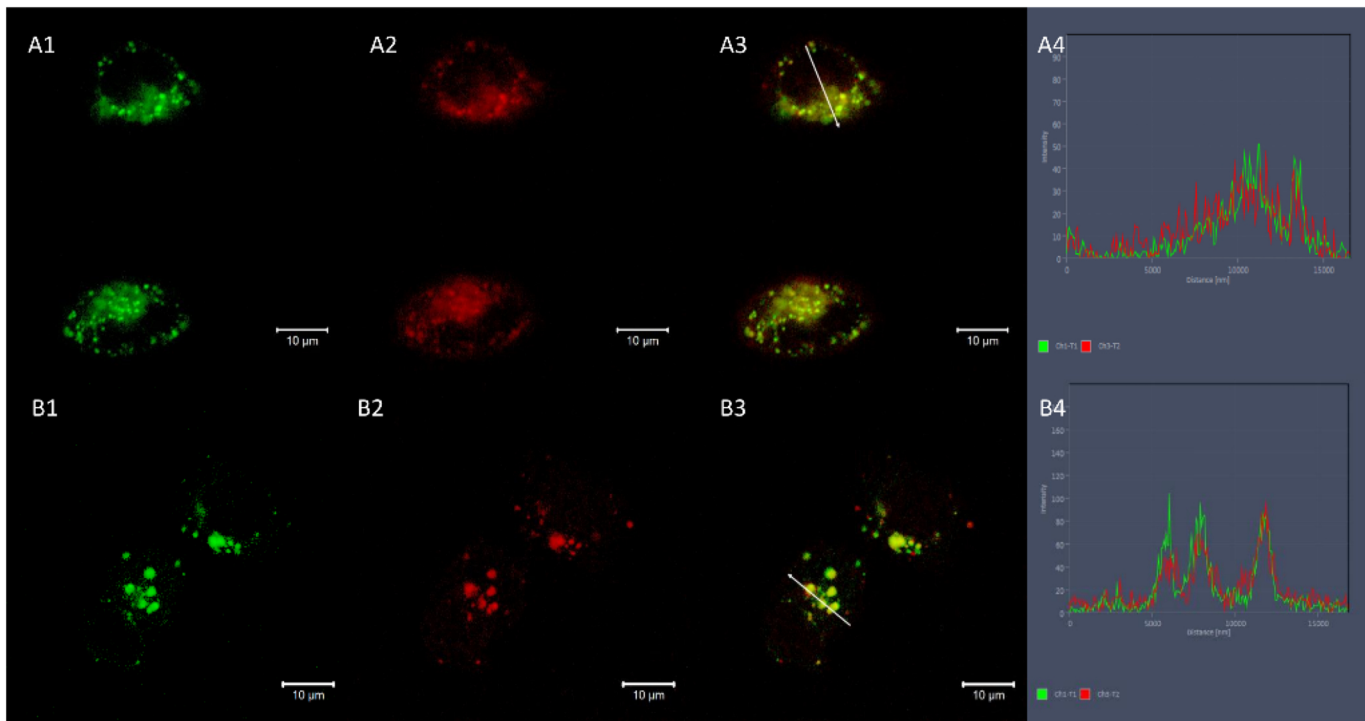


Figure 6

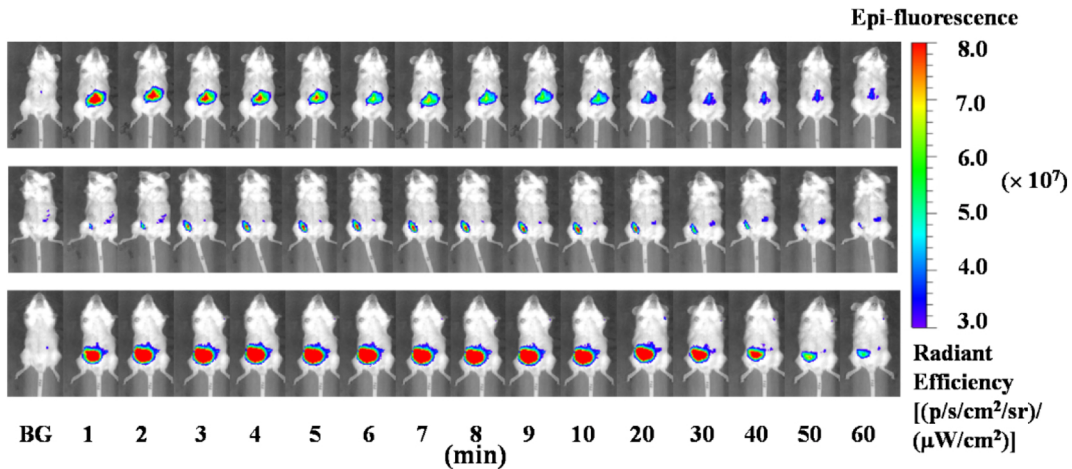


Figure 7